Resting and injury-induced inflamed periosteum contain multiple macrophage subsets that are located at sites of bone growth and regeneration

Resting and injury-induced inflamed periosteum contain multiple macrophage subsets that are located at sites of bone growth and regeneration

Kylie Anne Alexander[1,2], Liza-Jane Raggatt[1,2,3], Susan Millard[3], Lena Batoon[3] Andy Chiu-Ku Wu[1,2], Ming-Kang Chang[1], David Arthur Hume[1,4] and Allison Robyn Pettit[1,2,3]

1. The University of Queensland, Institute for Molecular Bioscience, St Lucia 4072, Australia.

2. The University of Queensland Centre for Clinical Research, Faculty of Medicine and Biomedical Sciences, Royal Brisbane Hospital, Herston, 4029, Australia.

3. Mater Research Institute-The University of Queensland, Translational Research Institute, Woolloongabba, 4102, Australia.

4. The Roslin Institute and Royal (Dick) School of Veterinary Studies, University of Edinburgh, Roslin, Midlothian EH25 9PS, Scotland, UK

Corresponding Author: Allison R Pettit. Mater Research Institute-The University of Queensland, Translational Research Institute, 37 Kent St, Woolloongabba QLD 4102, Australia Phone: +6173443 7575, Email: allison.pettit@mater.uq.edu.au

Running title: Periosteal macrophages in bone healing

Keywords: macrophages, osteomacs, periosteum, bone healing and bone injury.

Conflict of Interest: The authors declare no conflict of interest

Acknowledgments: This work was supported by National Health and Medical Research Council (NHMRC) project grant (631484) to ARP and LJR, NHMRC Dora Lush Biomedical Scholarship (409914) to KAA, a NHMRC Career Development Award (519744) to ARP, Australian and New Zealand Bone and Mineral Society Gap Fellowship to ARP and The Mater Foundation. The Translational Research Institute (TRI) Microscopy Core Facility contributed technical expertise and the TRI Biological Research Facility contributed to animal husbandry and monitoring.

Abstract

Better understanding of bone growth and regeneration mechanisms within periosteal tissues will improve understanding of bone physiology and pathology. Macrophage contributions to bone biology and repair have been established but specific investigation of periosteal macrophages has not been undertaken. We used an immunohistochemistry approach to characterise macrophages in growing murine bone and within activated periosteum induced in a mouse model of bone injury. Osteal tissue macrophages (osteomacs) and resident macrophages were distributed throughout resting periosteum. Tissues were collected from 4 week old mice and osteomacs were observed intimately associated with sites of periosteal diaphyseal and metaphyseal bone dynamics associated with normal growth. This included F4/80^{+}Mac-2$^{-/low}$ osteomac association with extended tracks of bone formation (modeling) on diphyseal periosteal surfaces. While this recapitulated endosteal osteomac characteristics, there was subtle variance in the morphology and spatial organization of modelling-associated osteomacs, which likely reflects the greater structural complexity of periosteum. We also demonstrated that osteomacs, resident macrophages and inflammatory macrophages (F4/80^{+}Mac-2^{hi}) were associated with the complex bone dynamics occurring within the periosteum at the metaphyseal corticalization zone. These 3 macrophage subsets were also present within activated native periosteum after bone injury across a 9 day time course that spanned the inflammatory through remodeling bone healing phases. This included osteomac association with foci of endochondral ossification within the activated native periosteum. These observations confirm that osteomacs are key components of both osteal tissues, in spite of salient differences between endosteal and periosteal structure and that multiple macrophage subsets are involved in periosteal bone dynamics.

Introduction

Macrophages have broad functional potential as a consequence of their heterogeneity, microenvironmental awareness and plasticity. To harness the potential of macrophage biology for improving human health, more refined characterisation of macrophage subsets in any given biological response is needed. We previously characterized the resident macrophages within bone, osteal tissue macrophages (osteomacs) with minimum identification criteria being $F4/80^{+}Mac\text{-}2^{-/low}$ cells within 3 cell diameters of a bone surface [1,2]. Osteomacs [1-8] and/or recruited inflammatory macrophages [4, 5, 9-13] can influence bone dynamic events, particularly bone forming osteoblast anabolic outcomes. Macrophages have also been shown to be associated with sites of pathologic bone loss including prosthetic joint loosening [14] and have been implicated in systemic bone loss in an animal model of osteoporosis [15]. Better appreciation of the full breadth of macrophage subtypes associated with bone dynamics and their bone-specific functional potential is required. Here we focused on macrophage contributions to skeletal biology and repair specifically in the periosteum.

The periosteum is a specialised connective tissue composed of a vascularized and innervated fibrous membrane that encapsulates bone. It has two layers: an outer fibrous capsule layer containing elastic connective tissue (including Sharpey's fibres), fibroblasts and blood vessels; and, an inner cambium layer containing capillaries, nerves, pre-osteoblasts/bone lining cells, osteoblasts and undifferentiated mesenchymal stromal/stem cells (also referred to as periosteum-derived progenitor cells) [16, 17]. Periosteal bone modeling is essential for long bone formation [17, 18] and also in bone accrual induced by mechanical loading [18, 19]. In contrast, the resting endosteum is a single cell layer of predominantly mesenchymal cells (osteoprogenitors, committed bone lining cells and mature osteoblasts) lining the internal surface of bone and is in

direct contact with adjacent bone marrow and sinusoidal network [20]. Endosteal composition and biology has been more thoroughly investigated compared to periosteum. These tissues can respond independently and often differently to the same stimuli (review in ref. 18). Progenitor cells within the endosteum and periosteum have different potential: endosteal progenitors are restricted to osteoblastic differentiation but periosteal progenitors have osteoblastic and chondrocytic bi-potential [21]. Therefore while many physiological bone dynamic processes occur in both endosteum and periosteum, they are distinct environments with varying biological mechanisms and outcomes.

We have reported that both resting endosteum and periosteum contain osteomacs [1]. We have provided detailed *in situ* characterization of osteomacs in both resting and active endosteal surfaces and provided insight into their bone-specific functions [1, 2, 22, 23]. We have not reported detailed characterization of periosteal osteomacs. Given the clear variance in tissue structure, cell constituency and osteochondroprogenitor cell characteristics [18], it is important to independently characterise periosteal osteomacs and their distribution.

The regenerative potential of periosteum is well described [16, 17, 21, 24] and this has been taken advantage of in many orthopaedic procedures (review in ref. 16). Given it is the major source of osteochondroprogenitor cells during fracture repair [21, 25], the regenerative potential of periosteum has been primarily assigned to these resident mesenchymal progenitor cells, with little consideration of the potential involvement of macrophages in this process [26, 27]. During normal fracture healing chondrogenesis and subsequently soft callus formation initiates within *de novo* granulation tissue that originates from the hematoma [4, 28]. The osteochondrogenic progenitors that are recruited to the hematoma-derived granulation tissue are likely sourced from the adjacent periosteum, that undergoes a proliferative response to the injury, and bone marrow

[28]. If formation of a hematoma is disrupted/delayed, successful bone repair still proceeds, but the anabolic response instead initiates within the fracture adjacent native periosteum [28]. Therefore understanding cellular mechanisms within native periosteum, as well as the *de novo* granulation tissue, will also be important for understanding bone repair and likely be more relevant in stress/hairline fracture [19, 29], periostitis and/or stabilized non-displaced simple fractures that often fail to cause hematoma formation. Anabolic initiation within the native periosteum may also participate in low energy fragility fracture healing [30].

In this study we characterized periosteal osteomacs and investigated the distribution of inflammatory versus resident macrophages, including osteomacs, within both naïve and inflamed periosteum using an established model of cortical bone healing (tibial injury model)[31]. The specific advantages of the tibial injury model is that it is minimally invasive (periosteum, endosteum and bone marrow left predominantly intact) [3, 31, 32] and therefore periosteal granulation tissue formation does not predominate the repair mechanism.

RESULTS

Periosteum in actively growing mice contains both osteomacs and resident macrophages

The distribution of long bone periosteal macrophages was examined in naïve, actively growing 4 wk old C57Bl/6 mice, with anti-F4/80 and anti-Mac-2 IHC performed in serial sections. The F4/80 antigen is a robust pan-macrophage marker in mouse tissues that is not expressed by osteoclasts [33, 34]. Mac-2 expression is indicative of activated/inflammatory macrophages [35], it is also expressed in osteoclasts [36] and chondrocytes [37]. Osteomacs were identified using our previously designated criteria: F4/80^{+}Mac-2$^{-/low}$ cells within 3 cells diameter of a bone surface [1, 38]. A comprehensive description of mouse long bones together with anatomical localization of different regions is presented in Supplemental Figure 1.

In actively growing bone, periosteal accrual on cortical diaphyseal bone surfaces occurs via bone modeling. This was easily identified in the actively growing 4 wk old bone using the mature osteoblast marker osteocalcin (Figure 1A). In a near serial section stained for F4/80 expression, numerous ramified osteomacs were observed intercalated within the mature osteoblasts (Figure 1B, arrows). This integrated patchwork pattern varied from osteomac distribution as sites of endosteal bone modeling where they have a more elongated morphology and form a more continuous canopy structure [1]. These modeling site-associated periosteal osteomacs were F4/80^{+}Mac-2$^{-/low}$ (Figure 1C & D), recapitulating their endosteal counterparts [1]. Periosteal osteomac/macrophage frequency was reduced in skeletally mature bone (10 wk old), particularly in the diaphyseal region (data not shown), which occurred in conjunction with previously reported age associated periosteal atrophy [30].

F4/80^{+} macrophages were also intercalated within metaphyseal periosteum, which is considerably thicker than diaphyseal periosteum particularly in actively growing bone [30]. The

metaphyseal corticalization zone during bone growth is a highly dynamic site with bone catabolism, modeling and remodeling occurring simultaneously in a focused anatomical location. Within the periosteum adjacent to the corticalization zone, F4/80^{+} macrophages were present in both the cambium and fibrous capsule layers (Figures 1E and G). Large ramified F4/80^{+}Mac-2$^{-/low}$ macrophages meeting the anatomical osteomac criteria were present in the cambium tissue close to the bone surface (Figure 1G and H, boxes). In addition to these bonafide osteomacs, two distinct resident macrophage populations were also identified. F4/80^{+}Mac-2$^{-/low}$ resident macrophages that were not anatomically adjacent to bone (Figure 1E-H, black arrows) and F4/80^{+}Mac-2^{high} activated macrophages (Figure 1E-H, grey arrows) resided in the outer cambium and capsule tissues. Co-localization of F4/80 and Mac-2 within periosteal activated macrophages in the corticalization zone was confirmed by double immunofluorescence staining (Figure 2 A-E).

It is assumed that these inflammatory macrophages have been activated as a consequence of aseptic mechanisms associated with bone growth including upregulation of 'pro-inflammatory' cytokines such as tumour necrosis factor [39]. Expression of Ly6C, an antigen associated with recruited inflammatory monocytes [40], was also examined in the naïve periosteum of 4 wk old mice and the vast majority of osteomacs/macrophages within periosteum did not express this marker (data not shown). Therefore metaphyseal periosteum contains both definitive osteomacs and at least two other resident macrophage populations.

Periosteal macrophage frequency was determined using flow cytometry assessment of periosteal single cell preparations that were isolated using and rapid enzyme free method to avoid enzyme-mediate antigen shedding. Successful isolation of periosteal cells was confirmed by 20 fold enrichment of CD45^{-}CD31^{-}CD51^{+} osteoblast in endosteal preparations compared to bone

marrow from contralateral limbs ($p < 0.002$, not shown). The percent frequency of $F4/80^{+}Ly6G^{-}$ macrophages was similar in periosteum (average 14%) and bone marrow (average 17%) preparations (Figure 2F), which is similar to the 16% macrophage frequency previously demonstrated in neonatal calvarial cell preparations [1]. Based on immunohistology examination above, osteomacs represent the largest portion or macrophages in the periosteal cell preparation.

Osteomacs, resident and inflammatory macrophages are present in inflamed periosteal tissue during the anabolic phase of bone healing *in vivo*.

The distribution of macrophages, including osteomacs, within the periosteum during a bone healing time course in a tibial injury model was investigated [3, 31]. This fully stabilized bone injury heals predominantly via intramembranous ossification forming an intra-medullar and inter-cortical bone bridge. It proceeds through standard repair stages of: inflammation phase (days 1 to 3), anabolic modeling phase (days 4 to 7), and a catabolic modeling/remodeling phase (days 8 to 12). It also induces a conservative periosteal anabolic reaction associated with the injury site, but does not proceed to periosteal bridging by a callus. The advantage of this model is that it only causes focal damage to the periosteum providing an opportunity to examine repair responses within the existing periosteum, which was identified by the presence of an intact fibrous capsule layer and clear presence of periosteal cambium layer.

During the early stages of anabolic repair 5 days post-surgery, gross morphological assessment showed granulation tissue had formed immediately above the injury site and was continuous with tissue meeting the description of native periosteum (Figure 2A, boxed area). The granulation tissue-inflamed periosteum transition occurred on average 500µm from either side of the cortical edge of the bone injury site. The injury-associated inflamed diaphyseal periosteum

was expanded (Figure 2) compared to resting periosteum (Figure 1C and [41]). This expansion was due to both inflammatory cell infiltrate and an increase in fibroblast and stromal-like cells (Figure 2). The inflamed periosteum contained three morphologically distinct strata: a cambium layer directly adjacent to bone surface; a superficial capsule layer; and, an inflammatory layer, situated between the cambium and the capsule (Figure 2B-F). Numerous F4/80^{+} cells were distributed throughout all 3 periosteal layers (Figure 2A and B), and many of the F4/80^{+} cells within the cambium were osteomacs (F4/80^{+}Mac-2$^{-/low}$; Figure 2B and C, arrows). The cambium also contained a small population of F4/80^{+}Mac-2^{high} inflammatory macrophages (Figure 2B and C, boxed area). Few, if any of the F4/80^{+} osteomacs/macrophages within the cambium expressed Ly6C (Figure 2D). The cambium robustly stained for type 1 collagen (Col1a1) with the majority of cells and extracellular matrix within this layer positively stained (Figure 2E). Expression of Col1a1 clearly demarked the cambium from the other layers (Figure 2B-F) and suggests that this layer is directly participating in the fibrous repair process.

The inflammatory layer of the expanded periosteum integrated directly with granulation tissue and contained F4/80^{+}Mac-2^{high} inflammatory macrophages (Figure 2B and C, circled area). These inflammatory macrophages were absent from the capsule (Figure 2B and C, grey arrows). The inflamed periosteum capsule macrophages were predominantly F4/80^{+}Mac-2$^{-/low}$Ly6C^{+} (Figure 2B, C and D, grey arrows). A subset of macrophages with the same marker profile was also observed in the inflammatory layer (Figure 2B, C and D). The majority of cells within the capsule layer were Ly6C^{+} (Figure 2D), including intercalated macrophages (Figure 2B-D, grey arrows), which was not observed in resting periosteum (data not shown). Overall, both osteomacs and inflammatory macrophages were prominent cellular components of the periosteal repair response throughout bone healing.

During late stage anabolic repair 7 days post-injury, the periosteal tissue associated with the injury zone remained expanded (Figure 3) compared to naïve diaphyseal periosteum (Figure 1). Numerous F4/80^{+} macrophages were present throughout the inflamed periosteum (Figure 3A, boxed area). Toluidine blue staining confirmed lack of proteoglycan rich cartilage and accordingly absence of endochondral callus formation (Figure 3B). Unlike day 5 post injury, the discrete inflammatory strata had resolved, leaving the 2 physiologic periosteal layers, which continued to be considerably thicker (Figure 3) than naive periosteum (Figure 1). F4/80^{+}Mac-2$^{-/low}$ osteomacs were located within the periosteal cambium layer and did not express Ly6C (Figure 3C, D and E, black arrows). There were a smaller number of F4/80^{+}Mac-2$^{+/high}$ inflammatory macrophages present within the periosteal cambium (Figure 3C and D, boxed area). F4/80^{+}Mac-2$^{+/high}$ inflammatory macrophages were also within the sub-capsular area of the fibrous capsule (Figure 3C and D, circled area). Small numbers of F4/80^{+}Mac-2$^{-/low}$Ly6C^{+} macrophages were still present in the superficial capsule (Figure 3C, D and E, grey arrows), although much lower levels of Ly6C antigen were expressed compared to day 5 (Figure 2). Col1a1 deposition was present throughout most of the periosteum at this time point although there was a clear gradient with higher expression closer to the cortical bone surface (Figure 3F). Interestingly at day 5 post surgery the capsule layer was negative for Col1a1 expression (Figure 2E). Col1a1 expression in the capsule layer coincided with capsule infiltration of F4/80^{+}Mac2$^{-/low}$Ly6C^{neg} resident macrophages (Figure 3).

Periosteal endochondral ossification was a late event occurring at the juncture of the wound induced granulation tissue and expanded endogenous periosteum.

At 9 days post-surgery the remodeling phase had initiated as evidenced by early stage excavation of the intramedullary bone bridge (Figure 4A and [3]). In many samples characteristics of the injury associated periosteum recapitulated those reported above for 7 days post-surgery (Figure 3). Toluidine blue staining combined with morphological features confirmed the presence of proteoglycan rich soft callus (Figure 4B, asterisk). Various stages of *de novo* bone formation were associated with the cartilage foci (Figure 4B and C, asterisk), from Col1a1 dense proteoglycan rich immature bone matrix (Figure 4B and C, circled areas) through to mature new bone (Figure 4B and C, crosshatch) that had been laid down on the original cortical surface (delineated by basophilic cement line in bone, Figure 4B, arrows). This pattern of matrix distribution supports that a conservative localized anabolic endochondral ossification response is induced within activated periosteum in this tibial injury model.

F4/80^{+}Mac-2$^{-/low}$ osteomacs were associated with new woven bone surfaces and particularly the immature Col1a1^{+} matrix (Figure 4D and E, black arrows). However, many of the F4/80^{+} cells in close proximity to these new bone surfaces co-expressed Mac-2 (Figure 4C-E, boxed area) and therefore it is unclear if they are osteomacs (osteomacs are Mac-2^{-} under physiologic conditions) that have become 'activated' or if they are inflammatory macrophages. F4/80^{+}Mac-2$^{+/high}$ inflammatory macrophages (Figure 4D and E, circled area) were also present within the cambium layer but predominantly restricted to Col1a1 low regions (Figure 4C-E). F4/80^{+}Mac-2$^{-/low}$Ly6C^{+} macrophages (Figure 4D, E and F, grey arrows) were present in the capsule region (Figure 4D, E and F, grey arrows). Ly6C can also be expressed by endothelial cells [42] and Ly6C^{+} cells were observed associated with a blood vessel bordering the cambium and capsule strata (Figure 4F). Overall multiple macrophage subsets are associated with anabolic foci within activated periosteum induced by bone injury.

DISCUSSION

A comprehensive characterization of periosteal cellular composition is needed to improve knowledge of growth-associated, adaptive and pathological bone dynamics as well as bone repair/regeneration[18]. Herein we definitively demonstrate that osteomacs and resident macrophages are distributed throughout resting periosteum. Osteomacs also intimately associate with sites of periosteal diaphyseal and metaphyseal bone modeling during normal growth. Periosteal osteomacs had a similar expression profile to endosteal osteomacs ($F4/80^{+}Mac\text{-}2^{-/low}Ly6C^{+/-}$) [1, 23], however their morphology and spatial organization varied subtly, which likely reflects the greater structural complexity of periosteum compared to endosteum. These observations confirm that osteomacs are key components of both osteal tissues, in spite of salient differences between endosteal and periosteal structure and adjacent environments. We also demonstrated that osteomacs ($F4/80^{+}Mac\text{-}2^{-/low}Ly6C^{+/-}$ cell within 3 cell diameters of bone surface), resident macrophages ($F4/80^{+}Mac\text{-}2^{-/low}Ly6C^{+/-}$ cell greater than 3 cell diameters of bone surface) and inflammatory macrophages ($F4/80^{+}Mac\text{-}2^{hi}$) were prominent cells within activated native periosteum after bone injury across a 9 day time course that spanned the inflammatory through remodeling healing phases. This included osteomac association with foci of endochondral ossification within the activated native periosteum.

Interestingly, osteomacs/resident macrophages were the prominent, but not exclusive, macrophage subtype in areas of high Col1a1 deposition in activated native periosteum induced by bone injury. Macrophage induction of collagen deposition, particularly during wound healing and fibrotic responses, is well documented [43]. Inflammatory macrophages potentially directly influence collagen deposition via expression of Mac-2 and, as Mac-2 can be secreted, their location within the immediate site of collagen deposition is not required [44]. The distribution of

Col1a1 staining within the cambium even raised the possibility that osteomacs and inflammatory macrophages within this tissue were actually expressing Col1a1, which was somewhat surprising but not unprecedented [45, 46]. Therefore, one of the functional contributions of osteomacs and other macrophage subsets within periosteum is likely stimulation of collagen deposition by mesenchymal cells, independent of whether they are osteoblasts or fibroblasts.

The presence of multiple macrophage subsets within active native periosteum induced by bone injury provides further weight to the necessity of more clear distinction between the independent functional roles of distinct macrophages subsets during bone growth and repair/regeneration. Macrophage functional transition has been suggested to be a key mechanism orchestrating appropriate progression through the multiple phases of repair in soft tissue wound healing [43]. We would predict that macrophage contributions would be even more intricate during the greater biological complexity involved in bone regeneration/healing. This is also supported by our description of resident and inflammatory macrophage site and phase specific distribution within granulation tissue during both intramembranous [3] or endochondral mediated bone repair [4]. The dynamic growth events at the metaphyseal corticalization zone also exhibited complexity in periosteal macrophage diversity during normal growth. This suggests that the highly specialized developmental events occurring within this dynamic site, which involves both bone formation and resorption acting in concert, requires diverse functional support from multiple specialized macrophage subsets.

Broad spectrum macrophage depletion resulted in rapid and striking loss of endosteal osteoblast surface and osteoblast-mediated bone formation [1, 2, 5, 6] and resulted in failed bone healing [3, 4]. Effort now needs to be focused on utilizing/developing more refined macrophage subset targeting approaches so a clear map of specific macrophage subset contributions can be

generated. Interestingly, in the tibial injury model exogenous CSF-1 induced selective expansion of osteomacs within the intra-medullar woven bone bridge and subsequently enhanced Col1a1 deposition at this site [3]. This provides evidence that even a broad spectrum pro-macrophage molecule can achieve subset specific outcomes and consequently have targeted and positive impact on bone repair.

A clear outcome of the current study is that osteomacs/macrophages are located at sites of periosteal anabolism and therefore it is likely that they contribute to the regenerative properties of periosteum. This needs to be confirmed by further investigation. Macrophage contributions to this regenerative potential have been considered for bone tissue engineering approaches [26, 27]. However, given the pleiotropic nature of macrophages, achieving appropriate and consistent promotion of macrophage trophic support of mesenchymal stem and progenitor cells, pro-angiogenic, chemotactic and regenerative cytokine/growth factor production versus inducing destructive/foreign body macrophage reactions may prove therapeutically challenging [26, 27]. Achieving the appropriate macrophage functional balance will be aided by fine mapping of macrophage subset specific contributions to periosteal anabolic and catabolic events and dissection of the molecules coordinating these outcomes. Our study also supports the previous suggestion [28] that anabolic events can initiate in the activated native periosteum adjacent to a fracture site. This suggests that fracture adjacent periosteum is a viable target organ for reigniting failed fracture repair and that promoting osteomacs/macrophages may be integral to achieving this approach.

This study confirms that osteomac/macrophage participation during bone homeostasis and anabolism, independent of the anabolic mechanism, are likely consistent in all osteal tissues. As we have also previously reported osteomac presence in calvarial osteal tissue [1] and others have

shown macrophage contributions to calvarial injury repair, this cellular mechanism applies to both flat and long bones. Our evidence that osteomacs are present in human osteal tissues [1, 47] provides support that this biology isn't a species specific phenomenon. Definitive dissection of the specific roles of macrophages and osteoblasts in bone formation and repair was recently revealed to be more challenging than traditionally appreciated as macrophage can be resistant to lethal doses of irradiation [48]. Therefore chimeric models are unlikely to conclusively distinguish macrophage versus mesenchymal contributions to bone biology or repair. Careful validation of osteoblast restricted promoter expression models is also required as our current and previous [44, 45] data suggest that macrophages can express Col1a1 [45, 46]. Overall the impact of osteomac/macrophage contributions needs to be carefully and appropriately considered during investigations of bone biology and bone repair.

METHODS

Animals

Animal experiments were undertaken as dictated by the Australian code for the care and use of animals for scientific purposes. The University of Queensland Molecular Biosciences and/or Health Sciences Ethics Committees approved all protocols involving animals. C57Bl/6 male mice were supplied from Australian Resource Centre (Canning Vale, WA, Australia) and MacGreen mice (express green fluorescent protein (GFP) transgene under the control of the *cfms* promoter resulting in expression in mature myeloid lineage cells including macrophages [49] were sourced from an in-house breeding colony. Sample size was dictated by previous published data [1,3,4] investigating macrophage contributions to bone biology and ethical considerations. No animals or samples were excluded from this study and were randomly allocated to different harvest points.

Periosteal Cell Enrichment and Quantification of Osteomac Frequency

Femora were harvested from 4-week old mixed gender MacGreen mice. Muscles surrounding the femora were removed by cutting the connective tissue from their attachment sites without scraping or damaging the periosteum. Epiphyseal bone ends were removed and central marrow was thoroughly flushed with 2% FBS/PBS using a 27G needle. Femora were cut in half longitudinally and the endosteal surface was gently flushed using a 19G needle and 2% FBS/PBS to dislodge any remaining endosteum and marrow. A periosteal enriched single cell suspension was generated using a gentle MACS Dissociator (Miltenyl Biotec, NSW, AU) as per manufacturer's instructions. Cells were washed and resuspended in 2% FBS/PBS to generate a

single cell suspension. Bone marrow was flushed from contralateral limbs using a 2% FBS/PBS and a 27G needle.

Bone marrow from the contralateral femur and periosteal cell preparation were blocked with 2% FCS/PBS. 1 x 10^6 bone marrow cells were incubated with myeloid or mesenchymal antibody cocktails for 40 minutes in ice on a rotary shaker. Myeloid antibody cocktail included anti-F4/80-Alexa647 (AbD Serotec, Kidlington, UK) and anti-Ly6G-PE/Cy7 (Biolegend). Mesenchymal antibody cocktail contained anti-Ter119-biotin (Biolegend), anti-CD31-BV605 (Biolegend), CD45-APC/Cy7 (Biolegend) and anti-CD51-PE (Biolegend). Specificity of staining was determined by comparison to unstained cells and appropriate isotype control cocktails. Cells were then washed and resuspended in 2% FCS/PBS. 5 µg/mL 7-amino actinomycin D (Life technologies, CA, USA) was added 10 min before flow cytometry analysis to allow exclusion of dead cells. Analysis was performed on Beckman Coulter's CyAn™ ADP Analyser (Beckman Coulter, Brea, CA). 300,000-1,000,000 events were collected and analysis performed on aggregate excluded, live cells using FlowJo software version 8.8.7 (Tree Star Data Analysis Software, Ashland, OR). Macrophages were gated as $F4/80^+Ly6G^-$ cells (not shown). After exclusion of $Ter119^+$ erythroid cells, osteoblasts were gated as $CD45^-CD31^-CD51^+$ cells.

Immunofluorescence Staining of Naive Bone Tissue

Dual immunofluorescence staining was performed on deparaffinized and re-hydrated sections from 4-week old C57Bl/6 mice (n = 7) using sequential staining with the following reagents: F4/80 (rat anti-mouse, Abcam, Cambridge, UK), goat anti-rat IgG $F(ab')_2$-biotin (Santa Cruz Biotechnology, CA), streptavidin conjugated-AlexaFluor647 (Thermo Fisher Scientific), Mac2 (rat anti-mouse) directly conjugated to AlexaFluor488, Biolegend, San Diego, CA). Nuclei

were counterstained with DAPI (4′,6-Diamidino-2-phenylindole dihydrochloride, Sigma Aldrich) and sections mounted with ProLong Gold mounting medium (Thermo Fisher Scientific). Slides were visualized using a Vectra-3 6-slide automated quantitative pathology imaging system (Perkin Elmer, Waltham, MA) and spectral unmixing performed using inForm software v2.2 (Perkin Elmer).

Statistical Analysis

Data is represented as mean ± SEM, an unpaired students T-test was used to analysis flow cytometry data using PRISM 5 (Graph pad software) and a p value of <0.05 was considered statistically significant.

Tibial bone injury model

11-12 week old male C57Bl/6 mice were used in the cortical tibial injury model [31] surgery was performed as previously described [31].

Tissue collection, processing and sectioning

All left hind limbs were collected and processed as previously described [3] from either naive 4 or 10 weeks (wk) old mice or mice subjected to tibial injury

Immunohistochemistry and histology

Immunohistochemistry (IHC) was performed on deparaffinized and re-hydrated sections at 3 sectional depths as previously described [1] with specific primary antibodies: F4/80 (rat anti-mouse, AbD Serotec, Kidlington, Oxford, UK), collagen type 1 (Col1a1; rabbit anti-mouse, US

Biological, Swampscott, MA), osteocalcin (rabbit anti-mouse, Alexix Biochemicals, San Diego, USA), Mac-2 (rat anti-mouse, eBioscience, San Diego, CA), and Ly6C (rat anti-mouse, Abcam, Cambridge, UK); or relevant isotype control antibodies (normal ratIgG2b (AbD Serotec), rat IgG2a (BD Bioscience Pharmingen, San Jose, CA) and normal rabbit IgG (Santa Cruz Biotechnology, Dallas, TX). All sections were counterstained using Mayer's hematoxylin (Sigma Aldrich) and mounted using permanent mounting media (Thermo Fisher Scientific, Waltham, MA). Toludine blue staining was carried out as previously described [4]. Tissue staining was viewed using a Nikon eclipse 80i microscope with a Nikon D5-Ri1 camera and NIS-elements imaging software version 3.1 (Nikon, Tokyo, Japan) or an Olympus BX50 microscope with an attached DP26 camera and imaged using Olympus CellSens standard 1.7 imaging software (Olympus, Japan).

References

1. Chang MK, Raggatt LJ, Alexander KA, Kuliwaba JS, Fazzalari NL, Schroder K *et al.* Osteal tissue macrophages are intercalated throughout human and mouse bone lining tissues and regulate osteoblast function in vitro and in vivo. *J Immunol* 2008; **181:** 1232-1244.

2. Winkler IG, Sims NA, Pettit AR, Barbier V, Nowlan B, Helwani F *et al.* Bone marrow macrophages maintain hematopoietic stem cell (HSC) niches and their depletion mobilizes HSCs. *Blood* 2010; **116:** 4815-4828.

3. Alexander KA, Chang MK, Maylin ER, Kohler T, Muller R, Wu AC *et al.* Osteal macrophages promote in vivo intramembranous bone healing in a mouse tibial injury model. *J Bone Miner Res* 2011; **26:** 1517-1532.

4. Raggatt LJ, Wullschleger ME, Alexander KA, Wu AC, Millard SM, Kaur S *et al.* Fracture healing via periosteal callus formation requires macrophages for both initiation and progression of early endochondral ossification. *Am J Pathol* 2014; **184:** 3192-3204.

5. Cho SW, Soki FN, Koh AJ, Eber MR, Entezami P, Park SI *et al.* Osteal macrophages support physiologic skeletal remodeling and anabolic actions of parathyroid hormone in bone. *Proc Natl Acad Sci U S A* 2014; **111:** 1545-1550.

6. Vi L, Baht GS, Whetstone H, Ng A, Wei Q, Poon R *et al.* Macrophages promote osteoblastic differentiation in-vivo: implications in fracture repair and bone homeostasis. *J Bone Miner Res* 2014; **30:** 1090-1102.

7. Guihard P, Boutet MA, Brounais-Le Royer B, Gamblin AL, Amiaud J, Renaud A *et al.* Oncostatin m, an inflammatory cytokine produced by macrophages, supports intramembranous bone healing in a mouse model of tibia injury. *Am J Pathol* 2015; **185:** 765-775.

8. Fernandes TJ, Hodge JM, Singh PP, Eeles DG, Collier FM, Holten I *et al.* Cord blood-derived macrophage-lineage cells rapidly stimulate osteoblastic maturation in mesenchymal stem cells in a glycoprotein-130 dependent manner. *PLoS One* 2013; **8:** e73266.

9. Xing Z, Lu C, Hu D, Yu YY, Wang X, Colnot C *et al.* Multiple roles for CCR2 during fracture healing. *Dis Model Mech* 2010; **3:** 451-458.

10. Lyons FG, Al-Munajjed AA, Kieran SM, Toner ME, Murphy CM, Duffy GP *et al.* The healing of bony defects by cell-free collagen-based scaffolds compared to stem cell-seeded tissue engineered constructs. *Biomaterials* 2010; **31:** 9232-9243.

11. Nicolaidou V, Wong MM, Redpath AN, Ersek A, Baban DF, Williams LM *et al.* Monocytes induce STAT3 activation in human mesenchymal stem cells to promote osteoblast formation. *PLoS One* 2012; **7:** e39871.

12. Guihard P, Danger Y, Brounais B, David E, Brion R, Delecrin J *et al.* Induction of osteogenesis in mesenchymal stem cells by activated monocytes/macrophages depends on oncostatin M signaling. *Stem Cells* 2012; **30:** 762-772.

13. Pirraco RP, Reis RL, Marques AP. Effect of monocytes/macrophages on the early osteogenic differentiation of hBMSCs. *J Tissue Eng Regen Med* 2013; **7:** 392-400.

14. Haynes DR, Hay SJ, Rogers SD, Ohta S, Howie DW, Graves SE. Regulation of bone cells by particle-activated mononuclear phagocytes. *J Bone Joint Surg Br* 1997; **79:** 988-994.

15. Cenci S, Weitzmann MN, Roggia C, Namba N, Novack D, Woodring J *et al.* Estrogen deficiency induces bone loss by enhancing T-cell production of TNF-alpha. *J Clin Invest* 2000; **106:** 1229-1237.

16. Ferretti C, Mattioli-Belmonte M. Periosteum derived stem cells for regenerative medicine proposals: Boosting current knowledge. *World journal of stem cells* 2014; **6:** 266-277.

17. Malizos KN, Papatheodorou LK. The healing potential of the periosteum molecular aspects. *Injury* 2005; **36 Suppl 3:** S13-19.

18. Allen MR, Hock JM, Burr DB. Periosteum: biology, regulation, and response to osteoporosis therapies. *Bone* 2004; **35:** 1003-1012.

19. Kidd LJ, Cowling NR, Wu AC, Kelly WL, Forwood MR. Bisphosphonate treatment delays stress fracture remodeling in the rat ulna. *J Orthop Res* 2011; **29:** 1827-1833.

20. Weatherholt AM, Fuchs RK, Warden SJ. Specialized connective tissue: bone, the structural framework of the upper extremity. *Journal of hand therapy : official journal of the American Society of Hand Therapists* 2012; **25:** 123-131; quiz 132.

21. Colnot C. Skeletal cell fate decisions within periosteum and bone marrow during bone regeneration. *Journal of Bone and Mineral Research* 2009; **24:** 274-282.

22. Winkler IG, Pettit AR, Raggatt LJ, Jacobsen RN, Forristal CE, Barbier V *et al.* Hematopoietic stem cell mobilizing agents G-CSF, cyclophosphamide or AMD3100 have distinct mechanisms of action on bone marrow HSC niches and bone formation. *Leukemia* 2012; **26:** 1594-1601.

23. Wu AC, Raggatt LJ, Alexander KA, Pettit AR. Unraveling macrophage contributions to bone repair. *BoneKEy Rep* 2013; **2**.

24. Yu YY, Lieu S, Lu C, Colnot C. Bone morphogenetic protein 2 stimulates endochondral ossification by regulating periosteal cell fate during bone repair. *Bone* 2010; **47:** 65-73.

25. Murao H, Yamamoto K, Matsuda S, Akiyama H. Periosteal cells are a major source of soft callus in bone fracture. *J Bone Miner Metab* 2013; **31:** 390-398.

26. Dong L, Wang C. Harnessing the power of macrophages/monocytes for enhanced bone tissue engineering. *Trends in biotechnology* 2013; **31:** 342-346.

27. Brown BN, Sicari BM, Badylak SF. Rethinking regenerative medicine: a macrophage-centered approach. *Frontiers in immunology* 2014; **5:** 510.

28. Ozaki A, Tsunoda M, Kinoshita S, Saura R. Role of fracture hematoma and periosteum during fracture healing in rats: interaction of fracture hematoma and the periosteum in the initial step of the healing process. *J Orthop Sci* 2000; **5:** 64-70.

29. Li GP, Zhang SD, Chen G, Chen H, Wang AM. Radiographic and histologic analyses of stress fracture in rabbit tibias. *Am J Sports Med* 1985; **13:** 285-294.

30. Fan W, Bouwense SA, Crawford R, Xiao Y. Structural and cellular features in metaphyseal and diaphyseal periosteum of osteoporotic rats. *J Mol Histol* 2010; **41:** 51-60.

31. Campbell TM, Wong WT, Mackie EJ. Establishment of a model of cortical bone repair in mice. *Calcified tissue international* 2003; **73:** 49-55.

32. Wu CA, Pettit AR, Toulson S, Grondahl L, Mackie EJ, Cassady AI. Responses in vivo to purified poly(3-hydroxybutyrate-co-3-hydroxyvalerate) implanted in a murine tibial defect model. *Journal of Biomedical Materials Research. Part A* 2009; **91:** 845-854.

33. Hume DA, Halpin D, Charlton H, Gordon S. The mononuclear phagocyte system of the mouse defined by immunohistochemical localization of antigen F4/80: macrophages of endocrine organs. *Proc Natl Acad Sci U S A* 1984; **81:** 4174-4177.

34. Hume DA, Loutit JF, Gordon S. The mononuclear phagocyte system of the mouse defined by immunohistochemical localization of antigen F4/80: macrophages of bone and associated connective tissue. *J Cell Sci* 1984; **66:** 189-194.

35. Novak R, Dabelic S, Dumic J. Galectin-1 and galectin-3 expression profiles in classically and alternatively activated human macrophages. *Biochim Biophys Acta* 2012; **1820:** 1383-1390.

36. Niida S, Amizuka N, Hara F, Ozawa H, Kodama H. Expression of Mac-2 antigen in the preosteoclast and osteoclast identified in the op/op mouse injected with macrophage colony-stimulating factor. *J Bone Miner Res* 1994; **9:** 873-881.

37. Ortega N, Behonick DJ, Colnot C, Cooper DN, Werb Z. Galectin-3 is a downstream regulator of matrix metalloproteinase-9 function during endochondral bone formation. *Molecular biology of the cell* 2005; **16:** 3028-3039.

38. Pettit AR, Chang MK, Hume DA, Raggatt LJ. Osteal macrophages: a new twist on coupling during bone dynamics. *Bone* 2008; **43:** 976-982.

39. Fernandez-Vojvodich P, Palmblad K, Karimian E, Andersson U, Savendahl L. Pro-inflammatory cytokines produced by growth plate chondrocytes may act locally to modulate longitudinal bone growth. *Hormone research in paediatrics* 2012; **77:** 180-187.

40. Robbins CS, Swirski FK. The multiple roles of monocyte subsets in steady state and inflammation. *Cell Mol Life Sci* 2010; **67:** 2685-2693.

41. Chang JS, Quinn JM, Demaziere A, Bulstrode CJ, Francis MJ, Duthie RB *et al.* Bone resorption by cells isolated from rheumatoid synovium. *Ann Rheum Dis* 1992; **51:** 1223-1229.

42. Alliot F, Rutin J, Pessac B. Ly-6C is expressed in brain vessels endothelial cells but not in microglia of the mouse. *Neuroscience letters* 1998; **251:** 37-40.

43. Novak ML, Koh TJ. Phenotypic transitions of macrophages orchestrate tissue repair. *Am J Pathol* 2013; **183:** 1352-1363.

44. Sharma UC, Pokharel S, van Brakel TJ, van Berlo JH, Cleutjens JP, Schroen B *et al.* Galectin-3 marks activated macrophages in failure-prone hypertrophied hearts and contributes to cardiac dysfunction. *Circulation* 2004; **110:** 3121-3128.

45. Vaage J, Lindblad WJ. Production of collagen type I by mouse peritoneal macrophages. *J Leukoc Biol* 1990; **48:** 274-280.

46. Fadini GP, Albiero M, Menegazzo L, Boscaro E, Vigili de Kreutzenberg S, Agostini C *et al.* Widespread increase in myeloid calcifying cells contributes to ectopic vascular calcification in type 2 diabetes. *Circ Res* 2011; **108:** 1112-1121.

47. Wu AC, He Y, Broomfield A, Paatan NJ, Harrington BS, Tseng HW *et al.* CD169(+) macrophages mediate pathological formation of woven bone in skeletal lesions of prostate cancer. *J Pathol* 2016; **239:** 218-230.

48. Hashimoto D, Chow A, Noizat C, Teo P, Beasley MB, Leboeuf M *et al.* Tissue-Resident Macrophages Self-Maintain Locally throughout Adult Life with Minimal Contribution from Circulating Monocytes. *Immunity* 2013; **38:** 792-804.

49. Sasmono RT, Oceandy D, Pollard JW, Tong W, Pavli P, Wainwright BJ *et al.* A macrophage colony-stimulating factor receptor-green fluorescent protein transgene is expressed throughout the mononuclear phagocyte system of the mouse. *Blood* 2003; **101:** 1155-1163.

Figure Legends

Figure 1: Resident macrophages and osteomacs are present in the periosteum of growing bone.

Representative images of periosteum in 4 wk C57Bl/6 murine long bone tissues (n = 5). All sections were counterstained with hematoxylin. A and B) IHC staining in near serial sections demonstrating that periosteal bone modeling tracks marked by osteocalcin^{+} (OCN) osteoblasts (A) contain frequently scattered F4/80^{+} osteomacs (B, black arrows). (C) F4/80^{+} osteomacs at diaphyseal periosteal modeling sites are Mac2$^{-/low}$ (D, black arrows). Serial section staining for F4/80 (E) or Mac-2 (F) expression demonstrated presence of multiple macrophage subsets in the periosteal metaphyseal corticolization zone. (G & H) magnification of left aspect of images in E and F respectively showing F4/80^{+}Mac-2$^{-/low}$ osteomacs (boxes), F4/80^{+}Mac-2$^{-/low}$ resident macrophages (black arrows) and F4/80^{+}Mac-2^{high} inflammatory macrophages (grey arrows). Original magnification: x40, with A, B, G and H digitally enlarged. CB (cortical bone). Scale bar indicates 50µm.

Figure 2: Activated macrophages reside within the periosteal corticalizaiton zone and periosteal and BM macrophages have similar tissue population frequency.

(A-E) Immunofluorescence double staining for F4/80 and Mac-2 expression in the periosteal corticalizaiton zone of 4-week old C57Bl/6 mice (n = 7). A) Pseudo-colouring of DAPI as haematoxylin counterstain and F4/80 staining as brown histology chromogen stain to provide anatomical context of corticalization zone. B-D) Immunofluorescence images with DAPI pseudo-coloured blue, (B and D) F4/80 expression pseudo-coloured red and (C and D) Mac-2 expression pseudo-coloured green and colocalisation of staining detected as yellow-orange staining (D). A-

D) Arrowheads indicate cells co-expressing F4/80 and Mac-2. E) Low power immunofluorescence image with DAPI pseudo-coloured white. Box indicates metaphyseal corticalization zone anatomical location of images shown in (A-D). A-D) Scale bar indicates 50 µm and (E) scale bar indicates 300 µm. A-D) Original magnification x40 and (E) original magnification x10. F) Flow cytometry analysis of periosteal (Periost) and bone marrow (BM) single cell preparations (n = 13) from 4-week old MacGreen mice to determine percent F4/80^{+} macrophages in live cells as an indication of macrophage frequency within these resident tissues. Error bars represent standard deviations and there was no significant difference between the two cell preparations.

Figure 3: Osteomacs and inflammatory macrophages are present within inflamed periosteum during the post-tibial injury early anabolic phase.

Representative images of periosteal injury sites 5 days post-tibial injury in 12 wk C57Bl/6 mice (n = 5). All sections were counterstained with hematoxylin. Within the periosteal injury zone, 3 distinct tissue layers were clearly evident based on morphological distinction: periosteal cambium (Cam), inflammatory (Inf) and capsule (Cap) layers. A) IHC staining with anti-F4/80 antibody (brown) demonstrating numerous F4/80^{+} cells distributed throughout the periosteal injury zone. Panels B-F are higher magnification images taken of the boxed area shown in A, in the same or serial sections stained for (B) F4/80, (C) Mac-2, (D) Ly6C, (E) Col1a1 expression and (F) matched RatIgG2b isotype control. The crosshatches denote the same anatomical landmark in each image. Numerous F4/80^{+} osteomacs (B, black arrows) were present within the cambium were confirmed to express minimal to no expression of Mac-2 (C, black arrows). The cambium also contained F4/80^{+}Mac-2$^{+/high}$ (B and C, box) inflammatory macrophages.

Expression of Ly6C in the cambium was minimal (D, black arrows). The inflammatory tissue contained numerous F4/80^{+}Mac-2$^{+/high}$ inflammatory macrophages (B and C, circled area) but also contained a population of F4/80^{+}Mac-2$^{-/low}$ resident macrophages, as there were more F4/80^{+} than Mac-2^{+} cells in this layer. The capsule tissue cells were predominantly Ly6C^{+} (D, grey arrows), some of which co-expressed F4/80 (B, grey arrows), but the capsule layer contained minimal to no Mac-2 staining (C, grey arrows). The cambium layer was Col1a1^{+} matrix enriched (E) with most cells in this layer expressing Col1a1^{+}. Specificity of staining confirmed using both RatIgG2b (F) and Rabbit IgG matched isotype control (data not shown). Original magnification: A x4 and B-F x20.

Figure 4: Macrophage, including osteomac distribution in periosteum during the post-tibial injury late anabolic phase.

Representative images of periosteal injury sites 7 days post-tibial injury in 12week C57Bl/6 mice (n = 5). All sections were counterstained with hematoxylin. Both periosteal cambium (Cam) and capsule (Cap) layers were morphologically discernible. A) IHC staining with anti-F4/80 antibody (brown) demonstrating F4/80^{+} cells distributed throughout both periosteal layers. Panels B-F are higher magnification images taken of the boxed area shown in A, in serial sections stained with (B) Toluidine blue, (C) anti-F4/80, (D) anti-Mac-2, (E) anti-Ly6C and (F) anti-Col1a1 antibodies. The crosshatch denotes the same anatomical landmark in each image. Toluidine blue staining confirmed absence of endochondral ossification at the selected periosteal injury site (B). Numerous F4/80^{+} cells present within the cambium were confirmed to be osteomacs (C, black arrows) due to their proximity to the bone surface and minimal to no expression of Mac-2 (D, black arrows). The cambium also contained F4/80^{+} (C, box), Mac-2^{+} (D, box) inflammatory

macrophages. Periosteal expression of Ly6C was minimal and primarily limited to low level expression in the capsule layer (E, black arrows) and scattered $Ly6C^{+}$ cells within the cambium with elongated endothelial morphology (E). The capsule layer contained numerous $F4/80^{+}$ (C) $Mac\text{-}2^{+}$ (D) inflammatory macrophages (circled area as example) and the superficial capsule contained a few cells $F4/80^{+}Mac\text{-}2^{neg}Ly6C^{+}$ (C, D and E, grey arrows). Both cambium and capsule contained $Col1a1^{+}$ matrix and cells with greater intensity of staining within the cambium (F). A and C-D were counterstained with hematoxylin. Original magnification: A x4 and B-F x20.

Figure 5: Osteomacs and macrophages are associated with periosteal endochondral ossification foci induce after tibial injury.

Representative images of endochondral ossification foci within periosteum 9 days post-tibial injury in 12 week C57Bl/6 mice (n = 5). A) IHC staining with anti-F4/80 antibody (brown) demonstrating $F4/80^{+}$ cells distributed throughout the periosteal injury zone. Panels B-F are higher magnification images taken of the boxed area shown in A, in serial sections stained for (B) Toluidine blue, (C) anti-Col1a1, (D) anti-F4/80, (E) anti-Mac-2 and (F) anti-Ly6C antibodies. The marked blood vessel (BV) serves as an anatomical landmark in each of these images. B) A Small foci of endochondral ossification is present 9 days post-tibial injury as indicated by the presence of proteoglycan rich cartilage (purple, *). Histological features also support that maturation of this cartilage to bone (cement line, arrows, with new bone above, light blue matrix marked with #) and adjacent proteoglycan rich osteoid (circles). C) This was confirmed to be new bone by staining for Col1a1 (brown), demonstrating intense staining for Col1a1 in the new bone (#) and immature osteoid (circles). Both $F4/80^{+}Mac\text{-}2^{-/low}$ osteomacs (D, E arrows) and

$F4/80^{+}Mac\text{-}2^{+/high}Ly6C^{-}$ inflammatory macrophages (D, E and F, boxed area) were observed adjacent to areas of new bone formation. The adjacent expanded periosteum contained numerous inflammatory $F4/80^{+}$ (D) $Mac\text{-}2^{+/high}$ (E) macrophages (circled area as example), which expressed minimal-low Ly6C (F). The capsule layer contained scattered cells expressing F4/80, Mac-2 and Ly6C (D-F, grey arrows). A and C-D were counterstained with hematoxylin. Original magnification: A x4 and B-F x20.

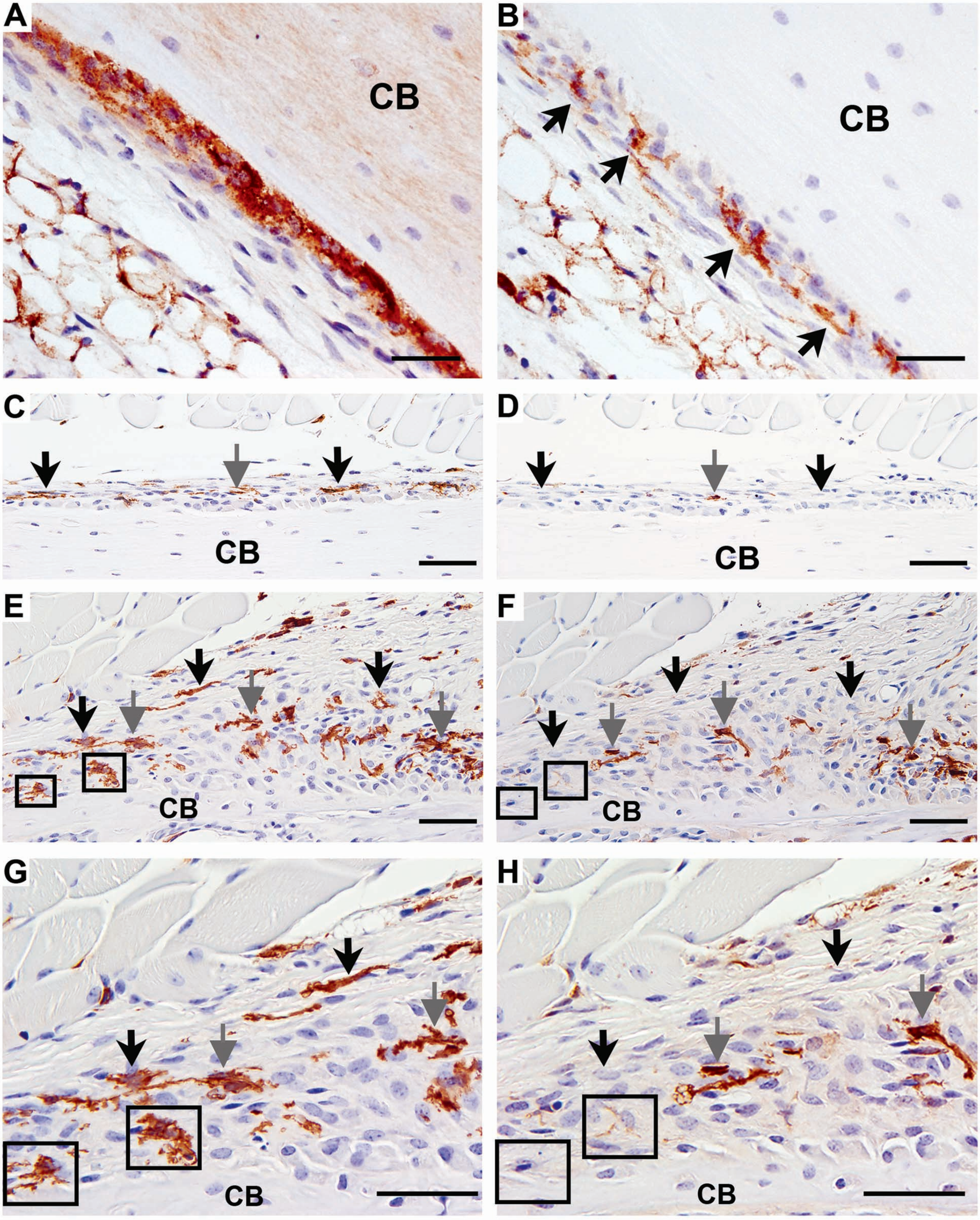
A
CB
B
CB
C
CB
D
CB
E
CB
F
CB
G
CB
H
CB

A F4/80 DAPI

B F4/80 DAPI

C Mac2 DAPI

D F4/80 Mac2 DAPI

E DAPI

F F4/80+ Macrophages

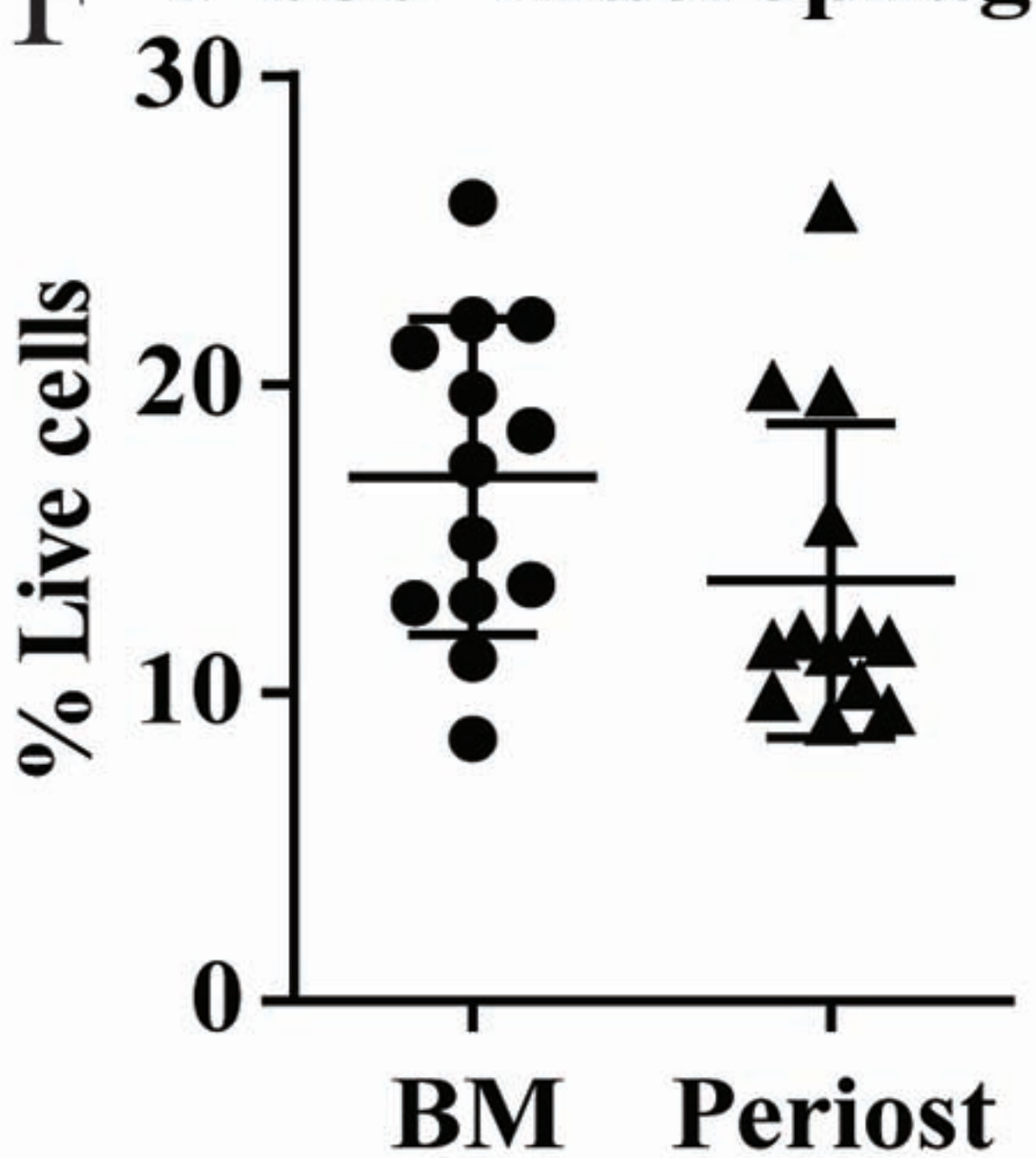

A

F4/80

B

F4/80

Cap

Inf

Cam

#

100 μm

C

Mac-2

D

Ly6C

E

Col1a1

F

RatIgG2b

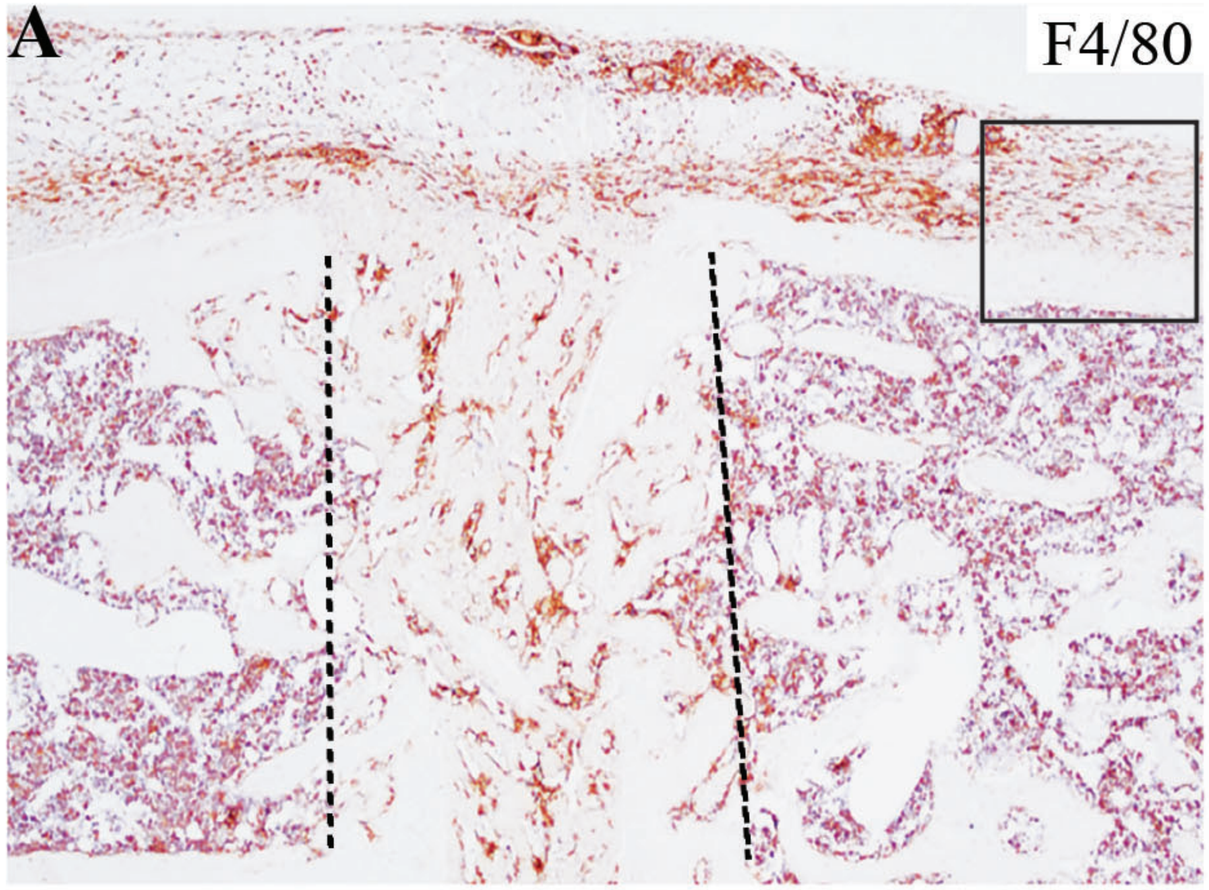
A
F4/80

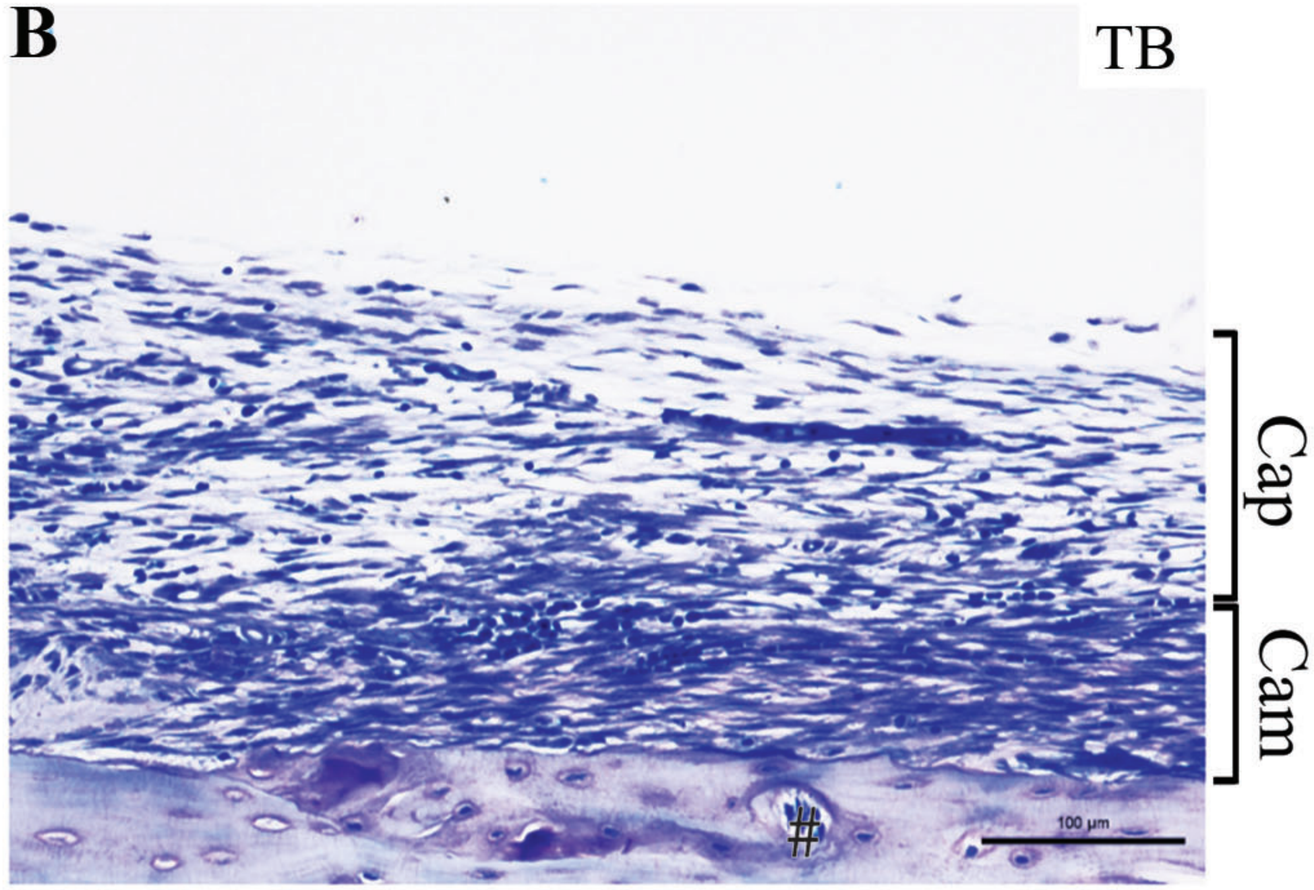
B
TB
Cap
Cam
#
100 μm

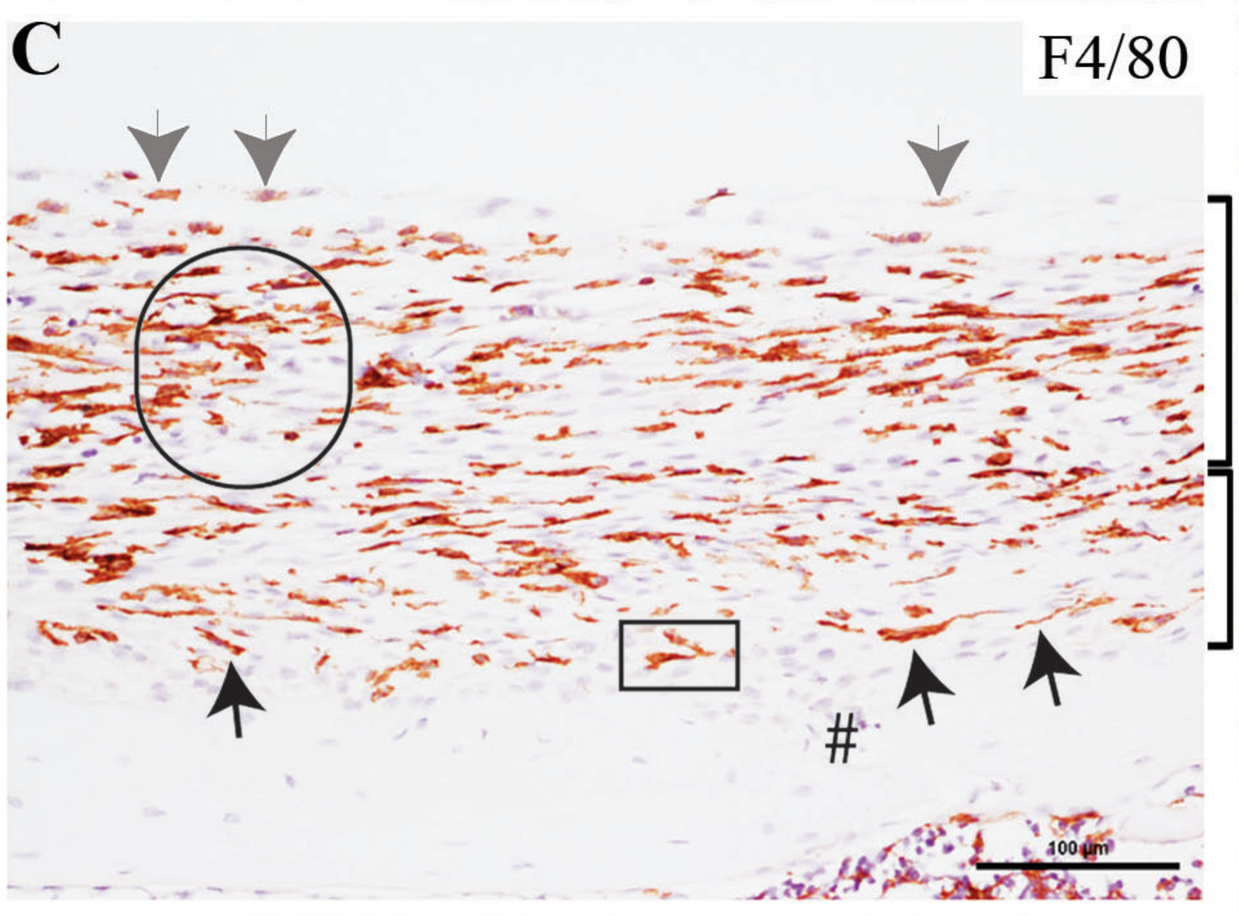
C
F4/80
#
100 μm

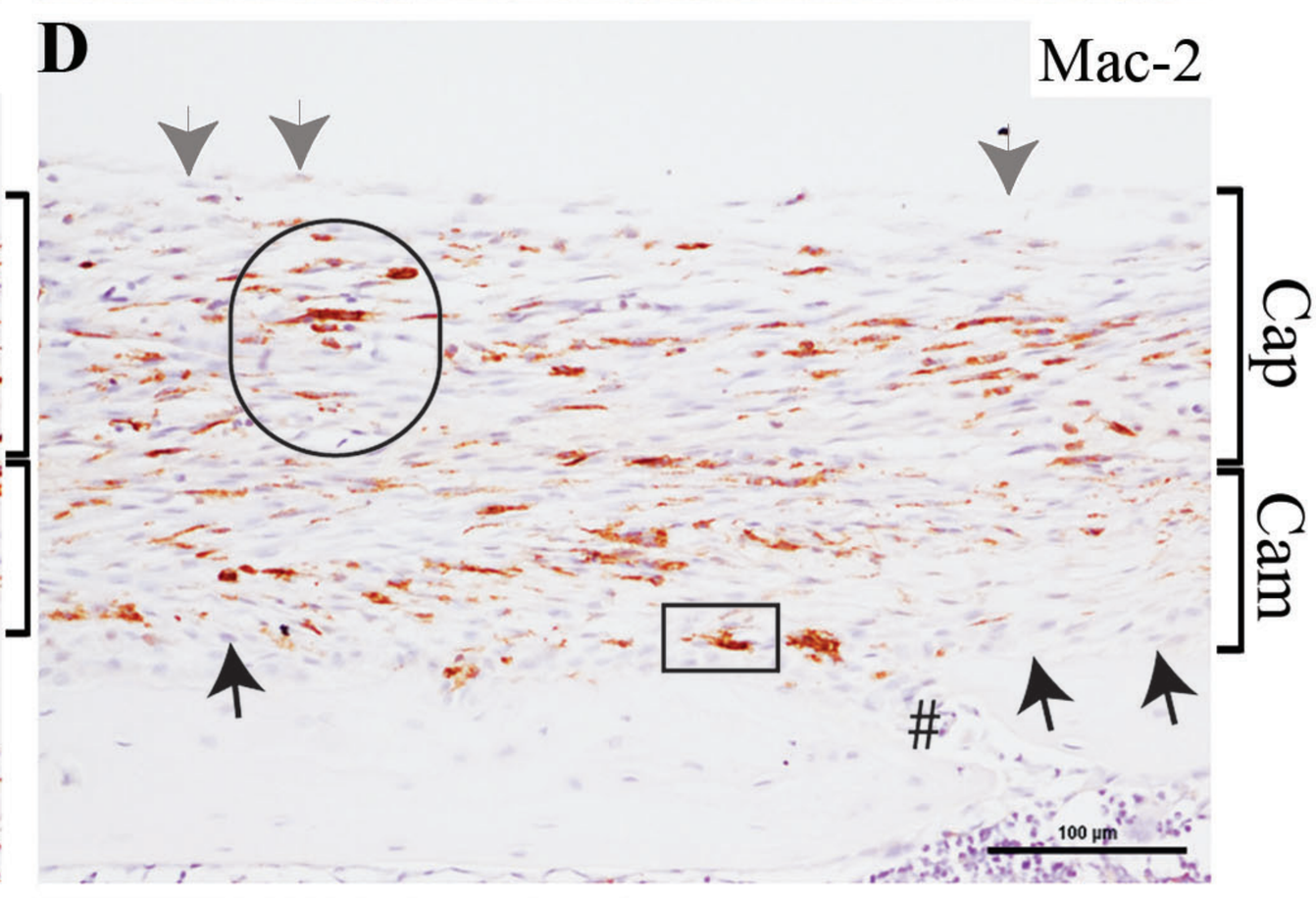
D
Mac-2
Cap
Cam
#
100 μm

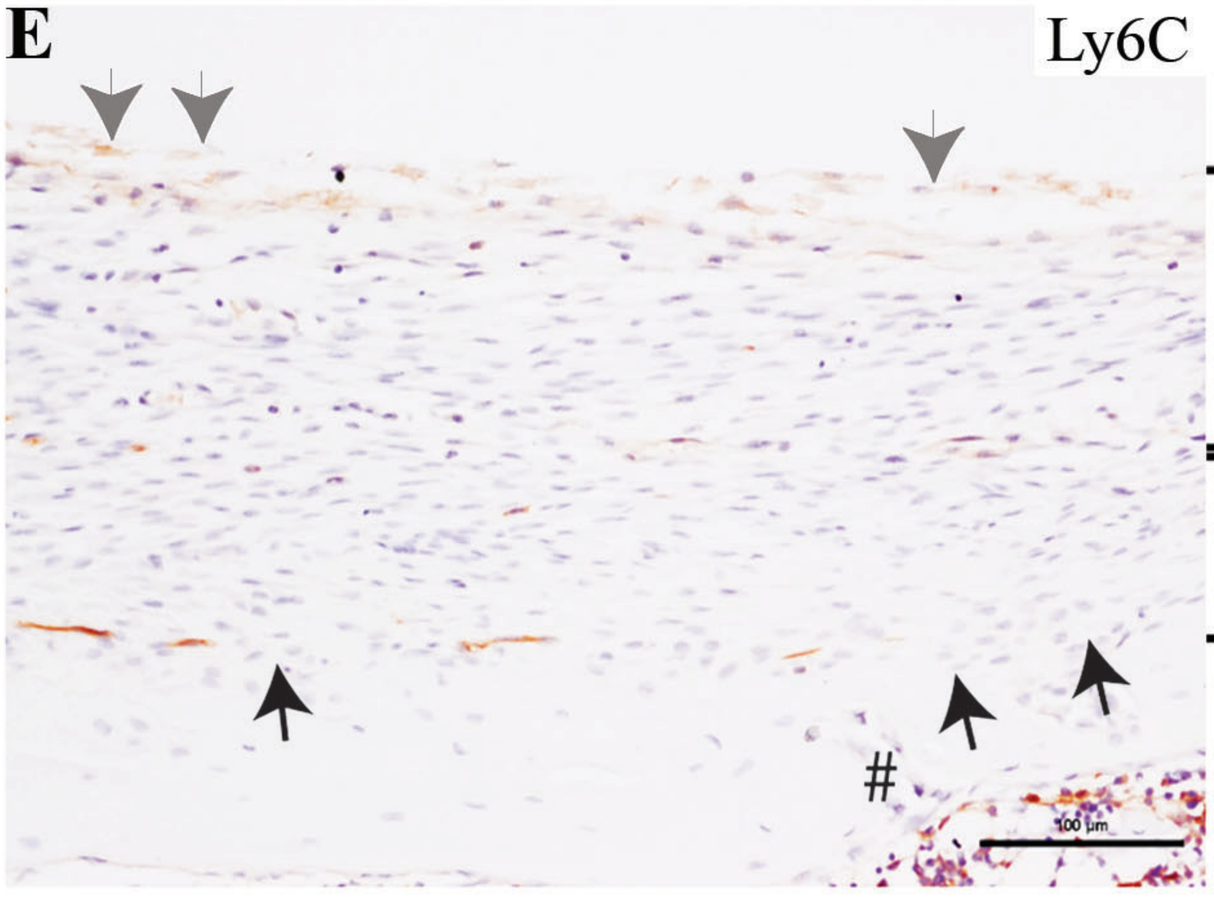
E
Ly6C
#
100 μm

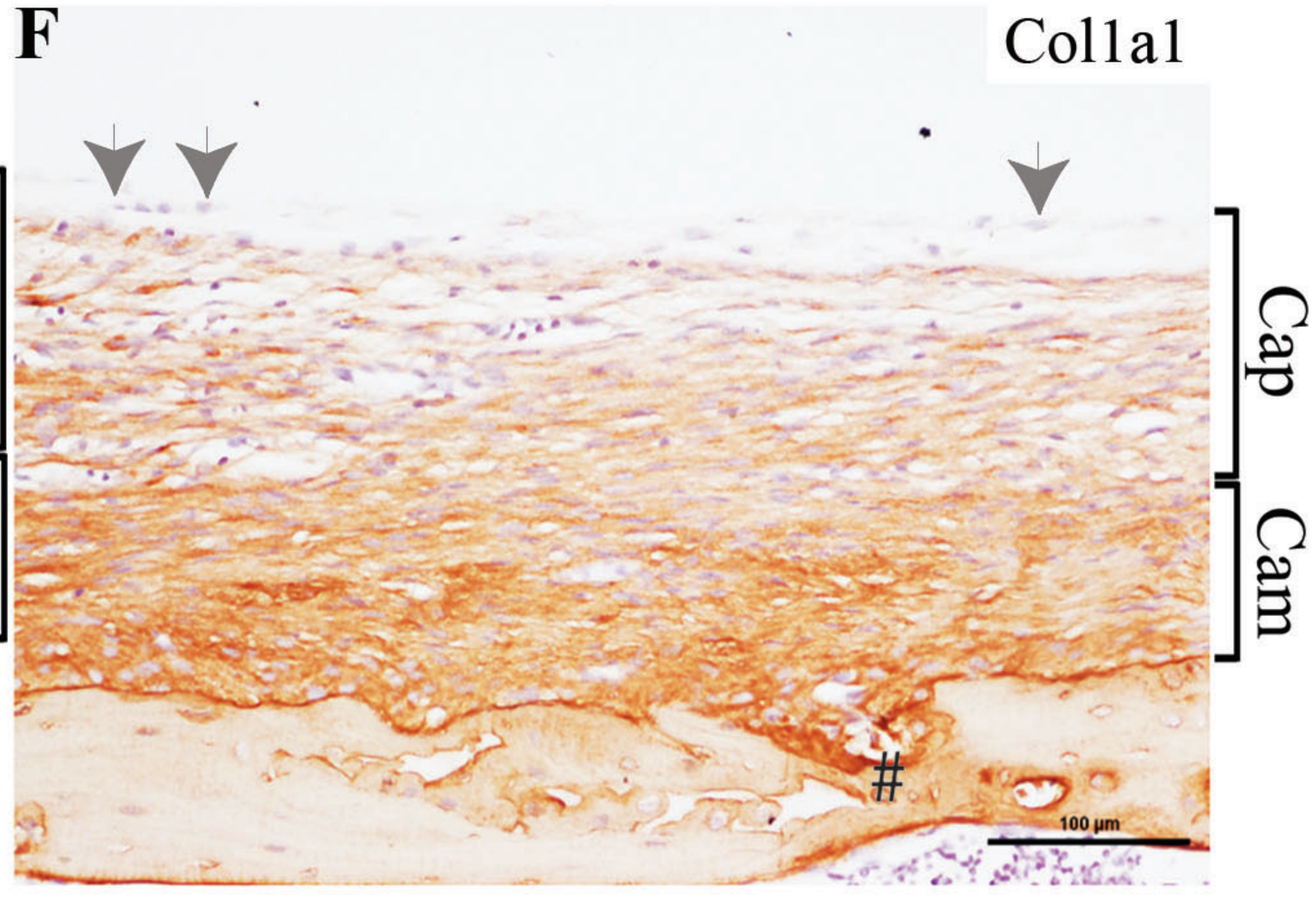
F
Col1a1
Cap
Cam
#
100 μm

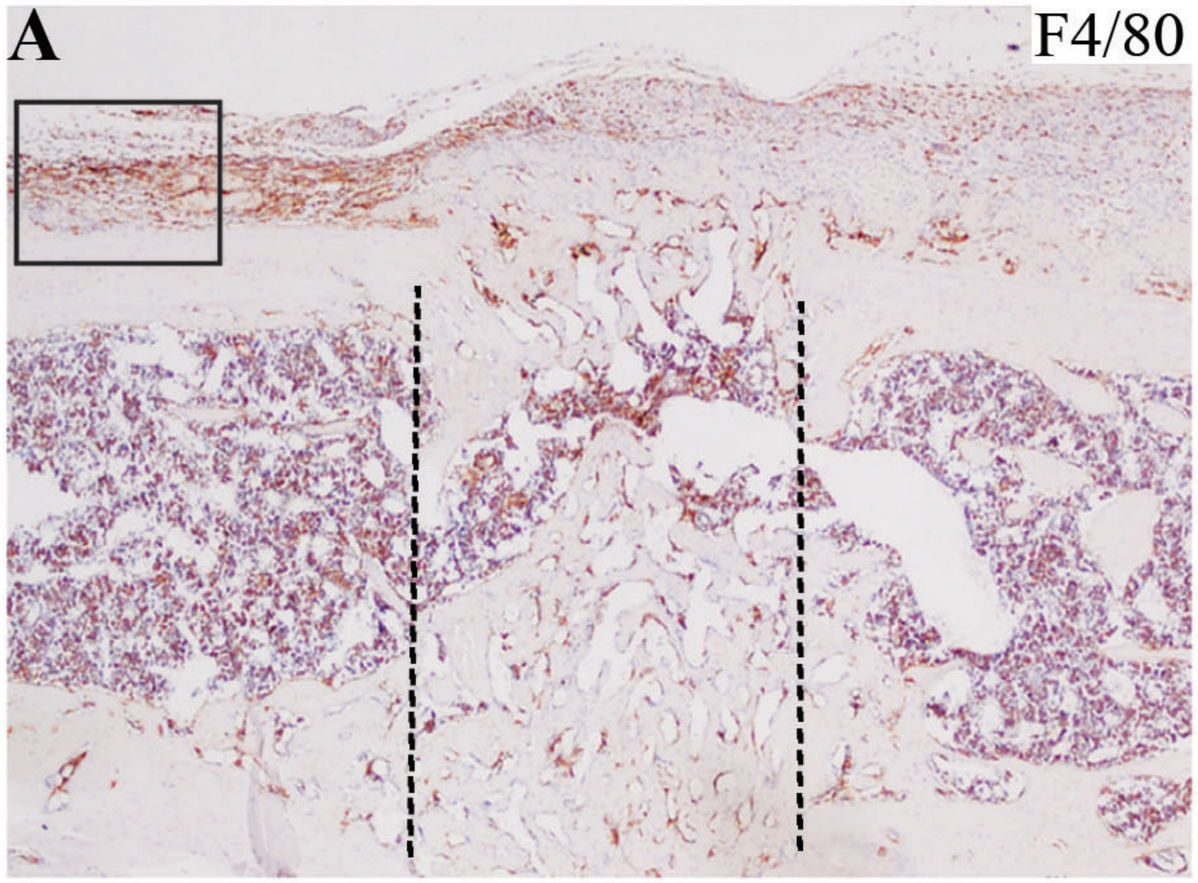
A
F4/80

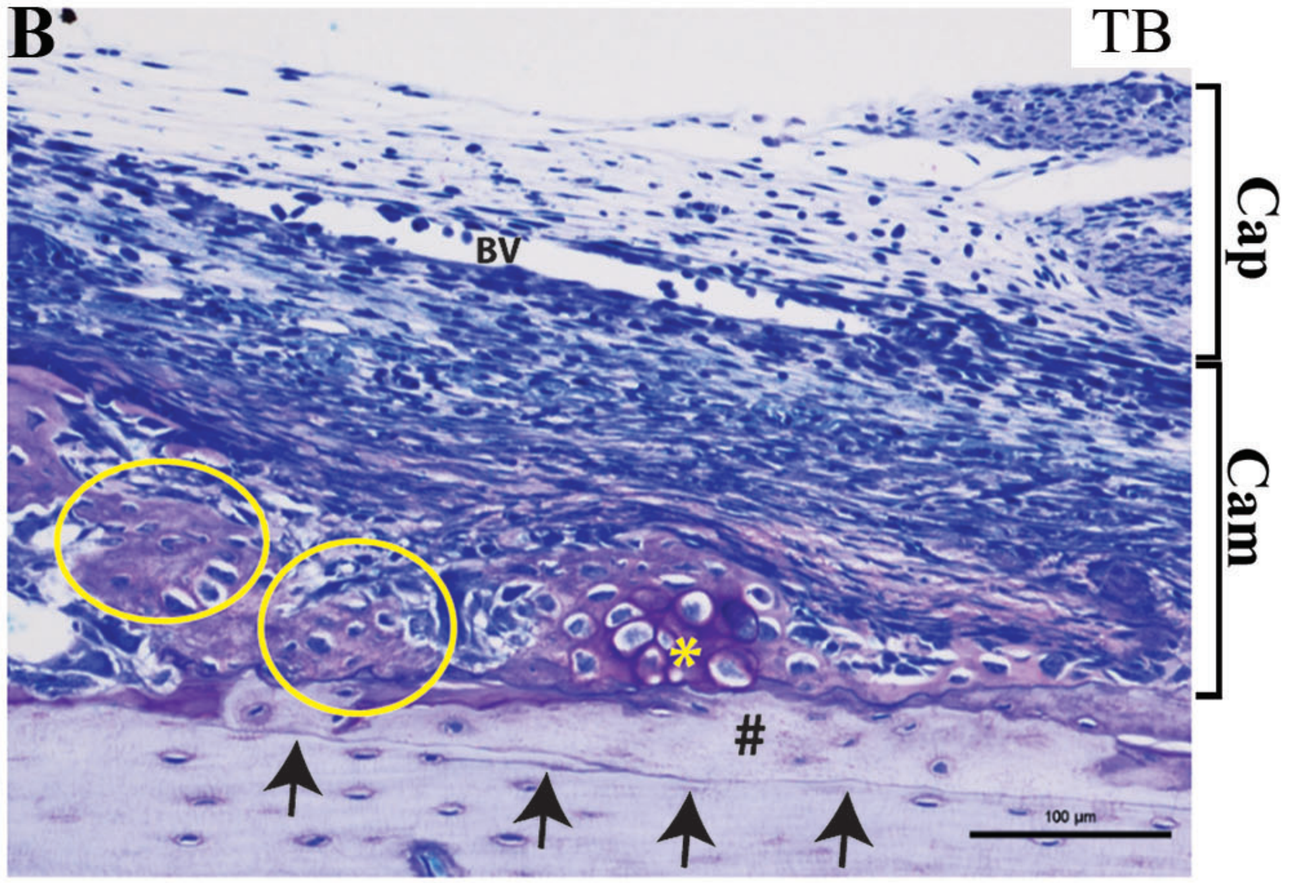
B
TB
BV
Cap
Cam
*
#
100 µm

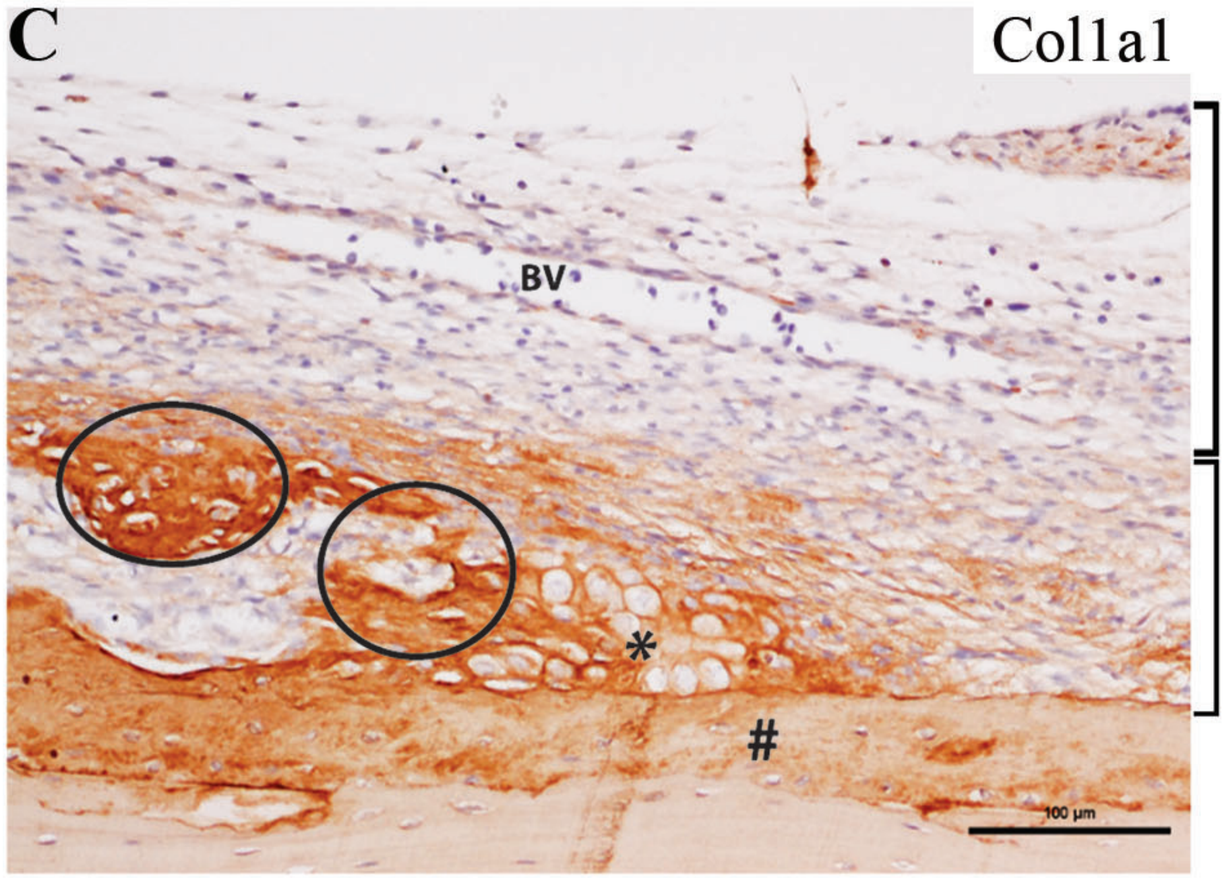
C
Col1a1
BV
*
#
100 µm

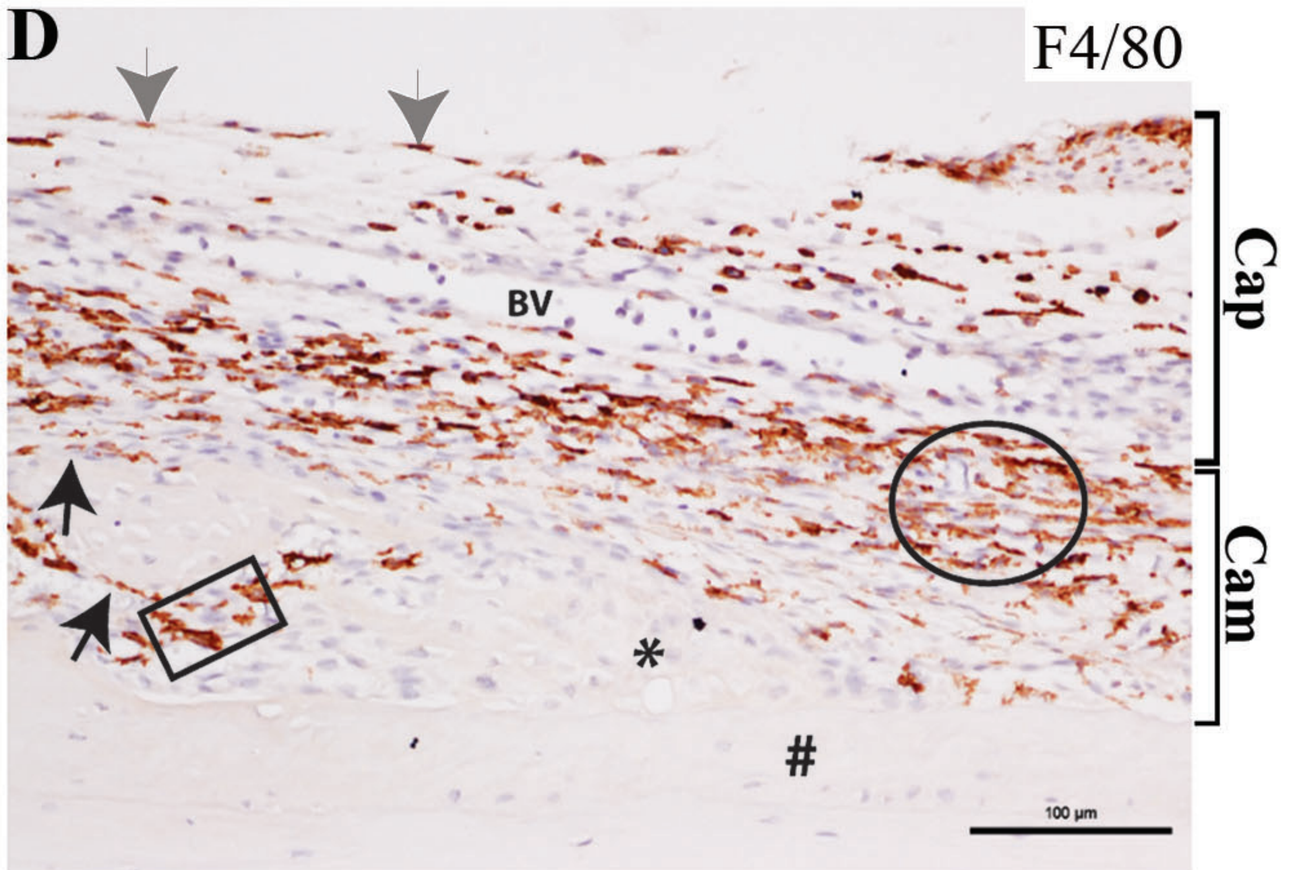
D
F4/80
BV
Cap
Cam
*
#
100 µm

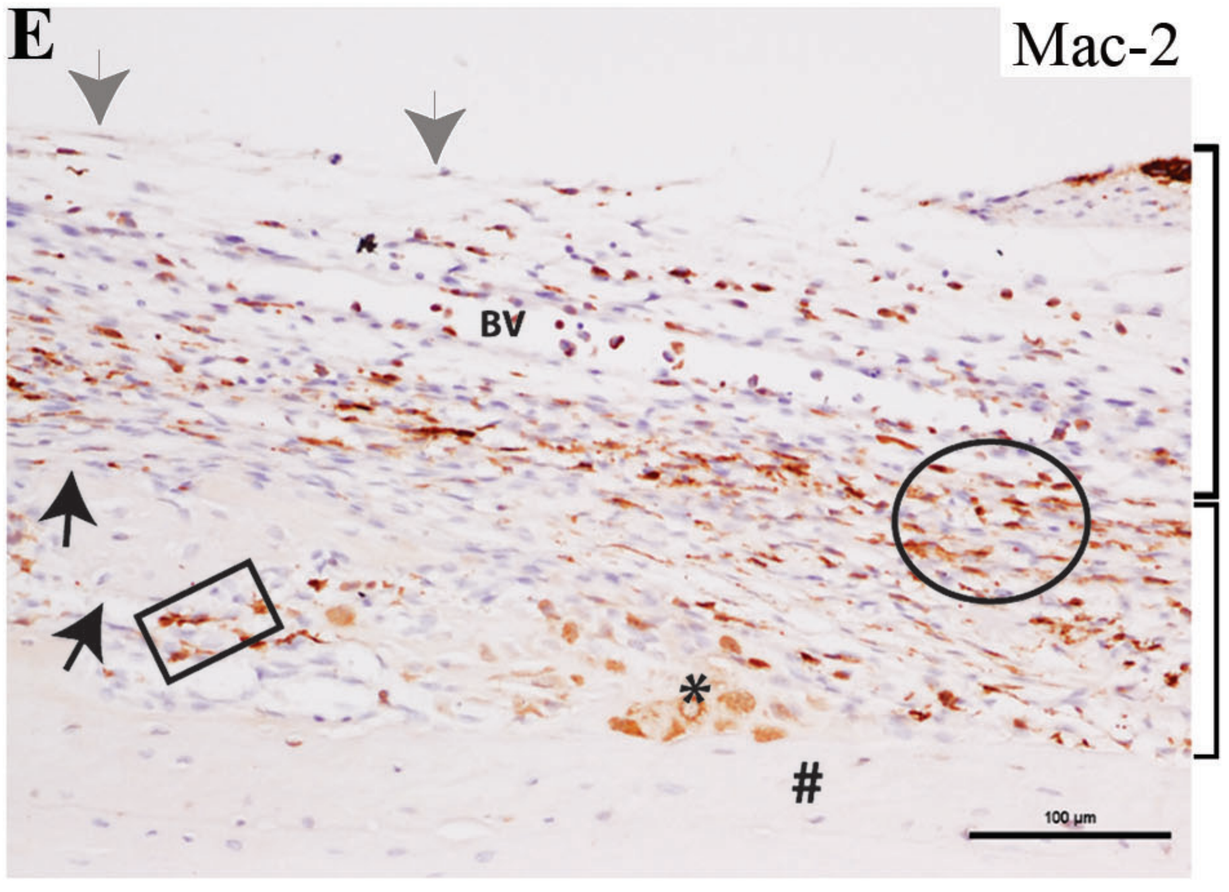
E
Mac-2
BV
*
#
100 µm

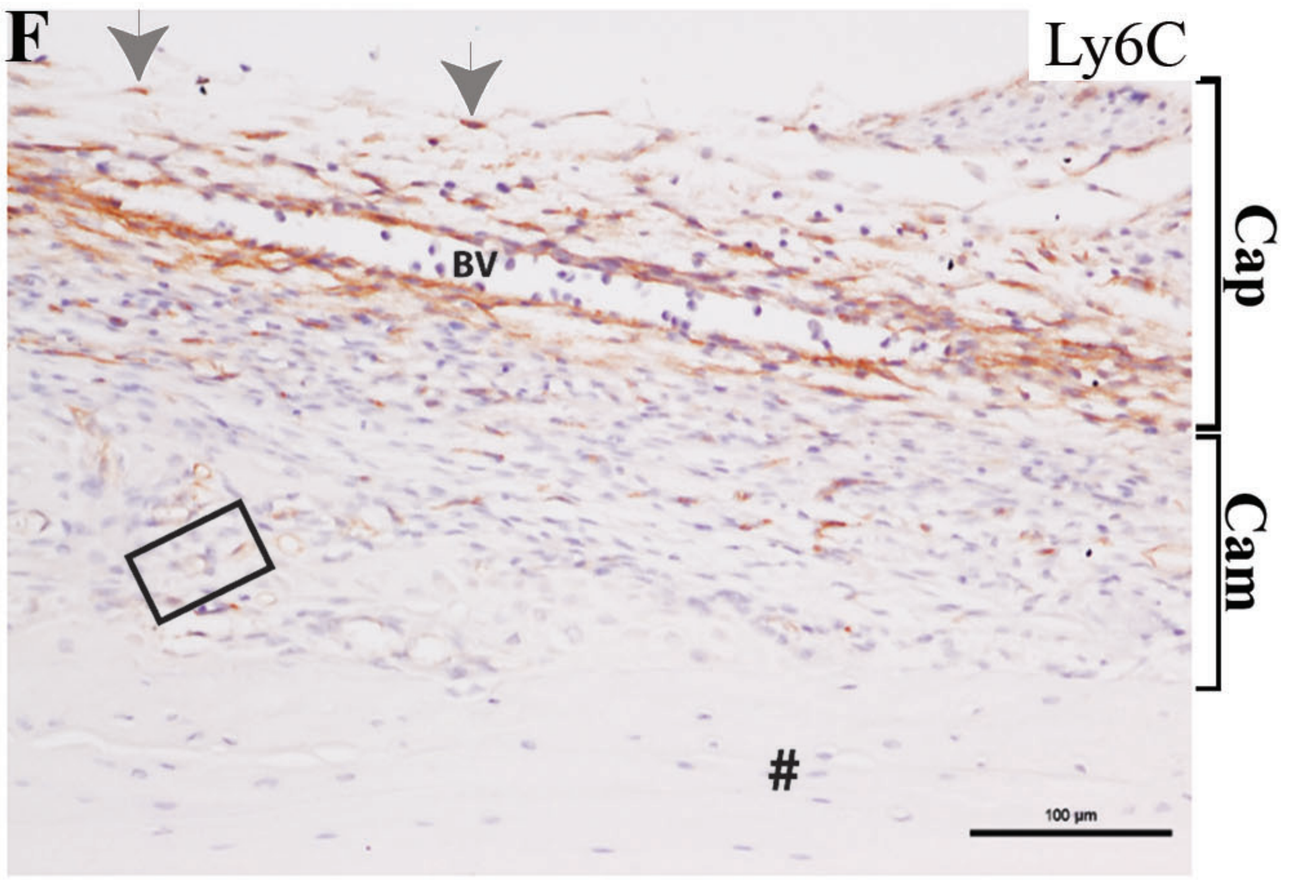
F
Ly6C
BV
Cap
Cam
#
100 µm